Review

New Nanomaterials and Luminescent Optical Sensors for Detection of Hydrogen Peroxide

Natalia A. Burmistrova [1,†], Olga A. Kolontaeva [1,2,†] and Axel Duerkop [2,*]

[1] Institute of Chemistry, Saratov State University, Saratov 410012, Russia;
E-Mails: naburmistrova@mail.ru (N.A.B.); kolontaevaoa@mail.ru (O.A.K.)

[2] Institute of Analytical Chemistry, Chemo- and Biosensors, University of Regensburg,
Regensburg 93040, Germany

[†] These authors contributed equally to this work.

[*] Author to whom correspondence should be addressed; E-Mail: axel.duerkop@ur.de;
Tel.: +49-941-943-4063; Fax: +49-941-943-4064.

Academic Editor: Igor Medintz

Abstract: Accurate methods that can continuously detect low concentrations of hydrogen peroxide (H_2O_2) have a huge application potential in biological, pharmaceutical, clinical and environmental analysis. Luminescent probes and nanomaterials are used for fabrication of sensors for H_2O_2 that can be applied for these purposes. In contrast to previous reviews focusing on the chemical design of molecular probes for H_2O_2, this mini-review highlights the latest luminescent nanoparticular materials and new luminescent optical sensors for H_2O_2 in terms of the nanomaterial composition and luminescent receptor used in the sensors. The nanomaterial section is subdivided into schemes based on gold nanoparticles, polymeric nanoparticles with embedded enzymes, probes showing aggregation-induced emission enhancement, quantum dots, lanthanide-based nanoparticles and carbon based nanomaterials, respectively. Moreover, the sensors are ordered according to the type of luminescent receptor used within the sensor membranes. Among them are lanthanide complexes, metal-ligand complexes, oxidic nanoparticles and organic dyes. Further, the optical sensors are confined to those that are capable to monitor the concentration of H_2O_2 in a sample over time or are reusable. Optical sensors responding to gaseous H_2O_2 are not covered. All nanomaterials and sensors are characterized with respect to the analytical reaction towards H_2O_2, limit of detection (LOD), analytical range, electrolyte, pH and response time/incubation time. Applications to real samples are given. Finally, we assess

the suitability of the nanomaterials to be used in membrane-based sensors and discuss future trends and perspectives of these sensors in biomedical research.

1. Introduction

The measurement of hydrogen peroxide (H_2O_2) concentrations is important in various points of view. First of all, monitoring of so-called reactive oxygen species that include e.g., singlet oxygen, H_2O_2, hydroxyl radicals, superoxide anions, or nitric oxide is of vital importance to control and understand numerous processes in biological systems. In recent years, various reports discussed the role of H_2O_2 in (patho)physiological processes [1–3], in oxidative stress [4] and as a messenger in cellular signaling [5–7]. The other reason of interest in H_2O_2 detection is the fact that the enzyme-activity of the huge class of oxidases or the concentration of their substrates or released products, respectively, can be measured via the amount of H_2O_2 produced. Finally, H_2O_2 is a widely used industry chemical. The current global production of hydrogen peroxide is millions of tons per annum and it is used in many areas including bleaching of wood pulp and paper, the treatment of industrial wastewaters and effluents, and in the food and pharmaceutical industry as a bleach and disinfectant.

It is therefore not surprising that numerous analytical approaches have been employed for quantitation of H_2O_2 in complex sample matrices including titrimetry, electrochemistry, chromatography and spectroscopy (photometry, chemiluminescence, fluorescence and phosphorescence). The state of electrochemical sensing of H_2O_2 was reviewed recently [8,9]. It has been shown that various types of electrochemical sensors can be used for fast measurements in both, the laboratory and the field. The specificity and sensitivity of the electrochemical sensors can be improved by the immobilization of enzymes or of nanoparticles on the surface of the electrode. Nevertheless, the application of electrodes is neither suitable for multiplexed measurements in high-throughput screening nor for intracellular assays or for *in vivo* imaging. The other drawback of electrochemical determinations of H_2O_2 is unreliability if other electroactive species are present in the sample.

In recent years, intensive research has evolved to design sensors that allow accurate and sensitive detection of H_2O_2 with high sensitivity and selectivity, that have a fast response, a simple setup and low-cost and are convenient to operate. Optical biosensors based on organic dyes and nanomaterials [10] that respond selectively to H_2O_2 are an attractive alternative for these purposes. Absorption, luminescence and chemiluminescence can be used as output signals to receive real-time and on-line information on the H_2O_2 concentration. On the one hand, this requires probes that optically respond to hydrogen peroxide. Those have been reviewed recently [11].

As a considerable amount of new probes for H_2O_2 based on luminescent nanomaterials have been published over the past years since the review of Schäferling *et al.*, we cover those in the first section of this review. The nanomaterial section is substructured into gold nanomaterials, polymeric and quantum dot nanomaterials, lanthanide nanomaterials and carbon nanomaterials. The most common detection format of these nanomaterials naturally is in solution in cuvettes but also a lateral flow assay

is shown and an assay where nanomaterials are stacked to a solid support made of a polydimethylsiloxane (PDMS) mold on a glass surface. Nanomaterials represent probes that are perspective with respect to a future use in optical luminescent sensors for H_2O_2 for continuous measurements.

However, while most of the nanomaterial probes are shown to be suitable for a single-use, the fabrication of an optical sensor requires considerably more knowledge in material chemistry to construct a system that works continuously and reversibly over time. Here, one needs to select appropriate materials to firmly embed the probe, prevent probe leaching and permit easy diffusion of the analyte to the receptor to warrant a short response time. Moreover, the receptor-transducer couple should work continuously over time in a real sample under potentially harsh conditions. Finally, the sensor should be inexpensive and have low production costs.

We therefore present the latest luminescent optical sensors for H_2O_2 in a second section of this review to open a perspective field for new applications of the nanomaterials referred to in the previous section. Most of the optical sensors presented are based on sensor membranes or sensor films and they are ordered in terms of the classes of the luminescent probes used as the receptor. Here, lanthanide complexes, metal-ligand complexes, oxidic nanoparticles and organic dyes are shown to reversibly work in solution over time. Moreover, several different formats are presented that range from the classical flow-through cell sensors (to continuously interrogate an analyte concentration e.g., in an analyte flow or in a by-pass of a bioreactor) to fiber-optic sensors with the film being immobilized at the tip of a fiber for high local resolution of concentration measurements. Finally, reusable sensor microplates are shown to offer a more green way to high-throughput measurements with less plastic waste incurred.

Commonly, new materials rapidly find their way into sensor development. Therefore, the merits of the nanomaterials are reviewed with respect to potential applications in sensors in a third section. Finally, we briefly discuss future trends and perspectives of these sensors in biomedical and bioanalytical research.

2. Probes for H_2O_2 Based on Nanomaterials

Recent developments in the field of nanotechnology have paved the way for numerous new materials with unique morphologies and physico–chemical properties to be used in sensor fabrication. Nanomaterials such as gold and silver nanoclusters, quantum dots, lanthanide-based nanoparticles, magnetic nanocomposites, polymeric nanoparticles and carbon materials have received enormous attention as promising tools in sensing of H_2O_2. The analytical figures of merits of H_2O_2 sensors and probes based on those types of nanomaterials are presented in Table 1.

Table 1. Optical Sensors and Probes for Hydrogen Peroxide Based on Nanomaterials.
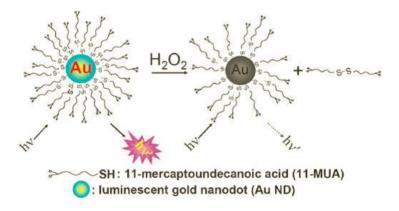
Material and Type of Nanostructure	Detected Signal	Analytical Range (LOD), μM	Incubation Time and Conditions	Application to Real Sample	Ref.
Gold Nanoparticles					
Au nanodots	Luminescence quenching of Au nanodots with 11-mercapto-undecanoic acid	0.1–1×10^3 (0.03)	10 min in 10 mM sodium phosphate buffer (PB) of pH 5.0 at 65 ℃	Glucose in serum sample	[12]
Dye-doped silica nanoparticles with Au nanoparticles on surface	Luminescence quenching of fluorescein isothiocyanate	0.1–15	10 min in 10 mM PB of pH 7.0 at 37 ℃	Detection of H_2O_2, hydroquinone, glucose, acetylthiocholine and paraoxon	[13]
Au nanoclusters stabilized by glutathione with peroxidase-like activity	Colorimetric and visual assay based on detection of oxidized 3,3′,5,5′-tetramethyl-benzidine (TMB)	1–10 (0.032)	15 min in 0.1 M PB of pH 6.0 at 30 ℃	Glucose in human serum	[14]
	Luminescence quenching of Au nanoclusters in presence of oxidized TMB	2×10^{-3}–6×10^{-4} (4.9×10^{-7})	15 min in 0.1 M PB of pH 6.0 at 30 ℃		
Au nanoclusters bioconjugated with Horseradish peroxidase (HRP)	Luminescence quenching of Au nanoclusters	0.1–100 (0.03)	10 min in 50 mM glycine buffer of pH 9.0 at 25 ℃		[15]
Polymer-Nanoparticles with Embedded Enzymes					
HRP co-entrapped with Texas Red-dextran inside porous polyacrylamide nanoparticles	Fluorescence quenching of Texas Red due to oxidation	1–25	5 min in 0.01 M phosphate-buffered saline (PBS) of pH 7.4	Cell culture medium containing 10% blood serum	[16]
Aggregation-Induced Emission Enhancement					
Fluorescent dye entrapped in CTAB micelles	Aggregation induced ratiometric (510/405 nm) fluorescence switched on by excited-state intramolecular proton transfer	up to 1×10^3	11 min in 0.3 mM CTAB solution (20 mM HEPES buffer of pH 7.4 at 25 ℃)		[17]
Quantum Dots					
Nanocomposites with Fe_3O_4 core and CdTe shell	Quenching of luminescence of quantum dots (QD) due to etching of surface	1×10^2–1×10^3 (35)	15 min in water	Human urine	[18]
CdTe@ZnS QDs conjugated to metal tetraamino-phthalocyanines (Metal: Al, Ni, Zn)	Increasing fluorescence of QDs	(9.8×10^{-3} 4.4×10^{-3} 2.2×10^{-3})	15 min in 50 mM PBS of pH 7.4 at RT		[19]

Table 1. *Cont.*

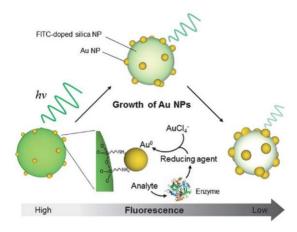| Material and Type of Nanostructure	Detected Signal	Analytical Range (LOD), μM	Incubation Time and Conditions	Application to Real Sample	Ref.
Lanthanide-Based Nanoparticles					
Poly(methyl methacrylate)-Eu^{3+} nanospheres	Luminescence quenching with biocatalytic growth of Au nanoparticles (AuNPs)	4.0–16 (2.0)	5 h growth of AuNPs in 0.01 M PBS of pH 7.05 in ice–water, luminescence after 20 min at RT		[20]
Coordination polymer nanoparticles (phenylalanine/Tb^{3+}) coordinated with carboxyphenyl-boronic acids	Quenching of fluorescence of nanoparticles due to intramolecular charge transfer from 4-oxo anions to emissive state of Tb^{3+}	$6–1 \times 10^3$ (2)	20 min in HEPES buffer of pH 7.0 at RT	Urine samples	[21]
Upconversion photoluminescence nanoparticles $NaYF_4$:Yb^{3+}/Er^{3+}	Quenching of luminescence of nanoparticles in presence of oxidized TMB	0.1–4.0 (0.045)	10 min in 0.02 M acetate buffer of pH 5.0 at 25 ℃	Glucose in human serum	[22]
Carbon Based Nanomaterials					
Carbon nanodots	Fluorescence quenching of nanodots in the presence of H_2O_2/Fe^{2+}	0.025–50 (0.01)	10 min in HCl of pH 3.0		[23]
Graphene quantum dots (GQDs) coupled with 2,2′-azino-bis(3-ethylbenzo-thiazoline-6-sulfonic acid (ABTS)	Absorbance change of ABTS	$10^2–10^4$ (20)	2 min in 10 mM Tris–HCl of pH 5.0 at 37 ℃		[24]
GQDs noncovalently labeled with hemin	Quenching of luminescence of GQDs	1–100 (0.1)	10 min in 20 mM PBS of pH 7.0 at RT	Glucose in human serum	[25]
Carboxyl-functionalized multiwalled carbon nanotubes	Fluorescence of tetraguaiacol formed from guaiacol oxidation in presence HRP	$(1.2 \ \mu M \times s^{-1})$	100 s		[26]

2.1. Gold Nanoparticles

Gold and silver nanoclusters have been widely used in biological sensing due to their low toxicity, excellent biocompatibility and stability, good solubility, and favorable luminescence properties [27,28]. Shiang *et al.* [12] fabricated water-soluble 11-mercaptoundecanoic acid-bound gold nanodots (11-MUA-AuNDs) of 2 nm size and applied them for highly selective and sensitive luminescent detection of H_2O_2 and glucose. In the presence of H_2O_2, 11-MUA units that are bound to AuNDs through Au–S bonding are oxidized to form an organic disulfide product (RS–SR), which is released into solution. The fewer 11-MUA molecules remaining bound to the AuNDs lead to a reduced luminescence. As a result, the presence of H_2O_2 induces a slight decrease in the absorbance at 375 nm and significant quenching of the luminescence of 11-MUA-AuNDs at 522 nm (Figure 1). The pH-optimum is 5.0 and a temperature of 65 ℃ provides a 10 min incubation time. The luminescence of 11-MUA-Au NDs can be restored upon adding of 11-MUA solution because new 11-MUA molecules are bound to the 11-MUA-Au NDs. Hence, a 10 times reusability of the luminescence quenching of the 11-MUA-AuNDs is observed after adding H_2O_2 and 11-MUA alternately and repeatedly. The nanodots could be used for the determination of glucose in a serum sample and showed a reusability of more than 10 times.
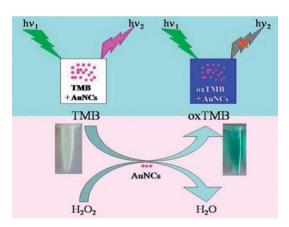

SH : 11-mercaptoundecanoic acid (11-MUA)
: luminescent gold nanodot (Au ND)

Figure 1. Schematic representation of 11-MUA-Au NDs responding to H_2O_2 based on the luminescence quenching by ligand release. Reproduced from [12] with permission of The Royal Society of Chemistry.

The absorbance increase, accompanied by the growth of gold nanoparticles (AuNPs) through the reduction of Au(III) ions in the presence of a reducing agent can quench the fluorescence of a dye if its emission spectrum overlaps with the absorbance spectrum of the AuNPs. This can be useful as an optical sensing platform for H_2O_2 and its enzyme-related analytes. For example, Lim *et al.* [13] synthesized fluorescein isothiocyanate (FITC)-doped silica nanoparticles (FSNs) with AuNP seeds. The fluorescence decrease caused by the growth of AuNPs on FSNs induced by the reducing reagent H_2O_2 is attributed to the inner filter effect of the AuNPs on the surface of the FSN on FITC emission at 520 nm. The utility of FSN-AuNPs as a facile platform for solid-phase optical biosensors by the development of multi-layer stacked FSN-Au NP on ultraviolet-ozone-treated glass slides was demonstrated (Figure 2).

Figure 2. Schematic diagram of Au NP enlargement-based detection of target analytes using the fluorescence change of FITC-doped silica NPs. Reproduced from [13] with permission of The Royal Society of Chemistry.

Ultra-sensitive colorimetric determination of H_2O_2 and glucose based on the intrinsic peroxidase-like activity of Au nanoclusters (AuNCs) stabilized by glutathione (GSH) was proposed by Zhao *et al.* [14]. The analyte concentrations are monitored indirectly via the color change of 3,3,5,5-tetramethylbenzidine (TMB) upon oxidation by H_2O_2 catalyzed by AuNCs. Here, the color change in an aqueous solution under visible light or photometry at 652 nm or the fluorescence resonance energy transfer between the AuNCs and oxidized TMB may be exploited for quantitation of H_2O_2 (Figure 3). The emission of the AuNCs can serve for quantitation of H_2O_2 down to picomolar concentrations and for glucose at nM levels.
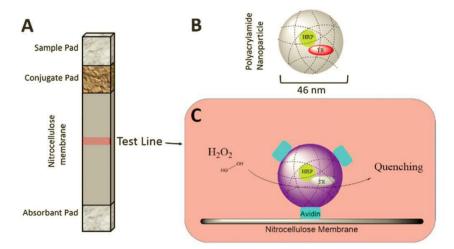

Figure 3. Schematic diagram of detection of H_2O_2 using the peroxidase-like activity of AuNPs. Reproduced from [14] with permission of The Royal Society of Chemistry.

A biochemical receptor/optical transducer scheme which can be used for a device permitting the continuous monitoring of a chemical compound in clinical or environmental samples should contain biochemical receptors that, in the appropriate concentration range, easily give reversible reactions and have autoindicating optical properties. Enzymes, mainly those having flavin or heme groups as cofactors have a potential for being used in this respect. In [15], the authors report horseradish peroxidase (HRP) functionalized fluorescent gold nanoclusters (AuNCs) via biomineralization. The

HRP retains its activity and the detection of H_2O_2 is accompanied by a decrease of the luminescence of the NCs at 650 nm and a small increase at 450 nm. Hence, H_2O_2 can be detected ratiometrically in the higher nM-μM range after 10 min incubation at pH 9. Other reactive oxygen species induce a similar response. The luminescence quenching at 650 nm is mostly due to the growth of AuNCs upon addition of hydrogen peroxide.

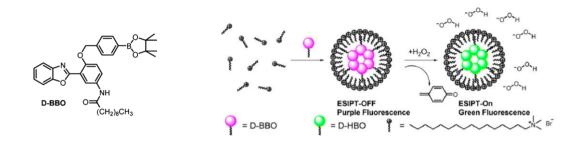## 2.2. Polymer-Nanoparticles with Embedded Enzymes

Analytical measurements using enzymes embedded in nano or microparticles have attracted great interest in various applications such as medical diagnosis, environmental monitoring and biological metabolite monitoring [29]. Here, the embedding of an enzyme (HRP) into a nanoparticle is combined with a lateral flow assay (LFAs) to improve the quality of signaling in LFAs when used with biological samples [16]. The rapid and sensitive LFA for quantification of H_2O_2 is based on HRP which is co-entrapped with Texas Red-dextran inside porous polyacrylamide NPs (Figure 4). The NPs were covalently immobilized on the test line of a lateral flow stripe (a nitrocellulose membrane) via avidin-biotin coupling. Texas Red dye (a rhodamine derivative) is oxidized by HRP/H_2O_2 and its luminescence is quenched ($\lambda_{exc} = 535$ nm, $\lambda_{em} = 600$ nm). The fluorescence readout of the LFA sensor was done in a commercial laser scanner. The LFA enables fast, selective, sensitive and point-of-care quantification of hydrogen peroxide in biological samples in concentrations of 1–25 μM. It was successfully demonstrated that enzyme and fluorophores (if protected in a porous NP) can advantageously work in enzyme-based LFA applications even in complex matrices like Dulbecco's Modified Eagle (DMEM) cell culture medium containing 10% blood serum.

Figure 4. (**A**) A typical lateral flow test strip with pads of sample, conjugate, absorbent and nitrocellulose membrane; (**B**) HRP enzyme and Texas Red dextran were entrapped inside a PAA nanoparticle of 46 nm in diameter; (**C**) Nanoparticle embedded HRP can oxidize Texas Red dye in the presence of hydrogen peroxide, when immobilized on the test line of a lateral flow strip via a protein linker. Reproduced from [16] with permission of The Royal Society of Chemistry.

2.3. Aggregation-Induced Emission Enhancement

A new ratiometric (510/405 nm) fluorescent probe for rapid detection of H_2O_2 via aggregation induced emission enhancement (AIEE) in surfactant buffer solution was designed, recently [17]. The authors use the modification of a traditional fluorophore (2-(2′-hydroxyphenyl)benzoxazole) exhibiting AIEE with a boronate based benzyl cleavable group. A C9-alkyl chain is included in the probe as the hydrophobic tail (Figure 5). Upon cleavage by H_2O_2 the probe D-HBO is obtained which can easily aggregate into particles of 195 nm size in a 0.3 mM cetyl trimethylammonium bromide (CATB) surfactant solution in 4-(2-hydroxyethyl)-1-piperazineethanesulfonic acid (HEPES) buffer (20 mM, pH 7.4, 25 °C) and emits green fluorescence (λ_{exc} = 341 nm) due to an excited-state intramolecular proton transfer (ESIPT). The D-BBO is encapsulated and restricted in rotation by the surfactant molecules. The cationic aggregates apparently accelerate the reaction (11 min incubation) of the probe with H_2O_2 at µM concentrations. Furthermore, D-BBO displays a highly selective response to H_2O_2 over other reactive oxygen species under identical conditions.

Figure 5. Structural formula of D-BBO and proposed mechanism for the detection of H_2O_2, based on an excited-state intramolecular proton transfer (ESIPT) process. Reprinted with permission from [17]. Copyright (2013) American Chemical Society.

2.4. Quantum Dots

Luminescent quantum dots (QDs) have been investigated in recent years as target-specific probes to develop various sensors and biosensors [30]. However, the separation and recovery of potentially toxic Cd-based QDs is difficult in practical applications. Multifunctional nanoprobes allow for combining the favorable properties of Cd-based QDs and of magnetic NPs. As a result, reusable QDs with a magnetic core can be produced to reduce the discharge of toxic NPs into the environment. This type of novel magnetic luminescent nanocomposites (Fe_3O_4@CdTe) have been successfully fabricated through layer-by-layer (LBL) self-assembly [18]. In the core–shell system, Fe_3O_4 nanoparticles have little impact on the luminescence signal from the surface of the CdTe QDs. H_2O_2 induces surface defects on the QD shell by chemically etching. The quenchiometric assay allows for quantitation of H_2O_2 in the higher µM-range. Although the quantitation range is comparatively high, the NPs can be easily separated after a reaction with a common magnet. Then, they are recycled by washing with water (attracted by a magnet) and released off the magnet into a new sample. This way, the NPs can be reused three times. Furthermore, the NPs were shown to enable glucose detection in human urine samples with red 651 nm luminescence (λ_{exc} = 450 nm).
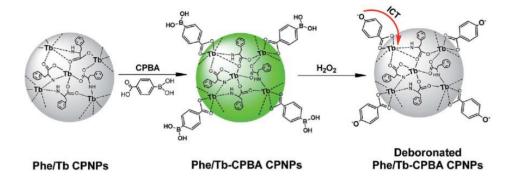
Nanoprobes for H_2O_2 sensing based on the covalent conjugation of different metal tetraamino-phthalocyanines (MTAPc: M = Al, Ni or Zn) to thiolated CdTe@ZnS QDs was developed by Adegoke *et al.* [19]. Upon coordination of the QDs to the MTAPc the luminescence of the linked QDs is switched off which is associated with Förster resonance energy transfer (FRET). H_2O_2 could switch on the luminescence of the linked QDs in a concentration-dependent manner because the FRET between the QDs and the MTAPc was disrupted. The order of the selectivity of the nanoprobes is: QD-NiTAPc > QD-AlTAPc > QD-ZnTAPc while the best limit of detection is offered by QDs-ZnTAPc (2.2 μM). The emission spectra were excited at 490 nm and the emission at 590 nm was found to concomitantly increase with the lifetimes (in the ns-range) in relation to the concentration of H_2O_2.

2.5. Lanthanide-Based Nanoparticles

The other major type of inorganic nanoparticles which are used for H_2O_2 sensing are lanthanide-based NPs [31]. Luminescence of lanthanide complexes is widely used in analytical applications because it displays unique properties like narrow bands of the emission spectra, a large Stokes' shift, high quantum efficiencies, and long lifetimes [32]. However, despite their good luminescence features, their sometimes poor water solubility, temperature-dependent emission and quenching of luminescence by water molecules have limited their practical applications. To overcome these disadvantages, some researchers have incorporated these complexes into various host matrices for preparing lanthanide-complex-based NPs.

The simple and effective solvent swelling method (also called the soaking method) was employed by Li *et al.* [20] for the incorporation of a europium complex into poly(methyl methacrylate) (PMMA-Eu). The Eu complex contained 2-thenoyltrifluoroacetone and isonicotinic acid in molar ratios of 1:3:1. The protocol for determination of H_2O_2 includes the formation of AuNPs upon reduction of Au(III) salts by H_2O_2 under the catalysis of Au nanoparticle seeds (in 0.01 M PBS, pH 7.05 in an ice-water bath for 5 h). The assay of H_2O_2 involves the fluorescence resonance energy transfer from the PMMA–Eu nanospheres to the AuNPs. The decrease of the luminescence intensity of the PMMA–Eu nanospheres at 612 nm (λ_{exc} = 365 nm) results from the changes in the concentrations of $HAuCl_4$ and Au nanoparticles (and their enlargement) during the growth process.

Coordination polymers constructed from metal ions and organic bridging ligands have recently emerged as very interesting functional materials due to their tunable structures and properties. In [21] functionalized lanthanide coordination polymer nanoparticles (CPNPs) were grown by a direct post-modification strategy to receive selectivity with respect to H_2O_2. The CPNPs contain terbium ions (Tb^{3+}) as metal nodes and phenylalanine (Phe) as bridging ligands. Then 4-carboxyphenylboronic acid (CPBAs) is coordinated to the free coordination sites of Tb^{3+} to yield a nanoparticular material. Upon the complexation of CPBA with parent CPNPs a strong green fluorescence (545 nm) of Tb^{3+} is observed (λ_{exc} = 240 nm). The addition of H_2O_2 in μM-mM concentrations probably hydrolyses the boronic acid group of CPBA and a 4-oxo anion at the CPBA residue is formed. The intramolecular charge transfer process from the formed 4-oxo anions to the emissive state of Tb^{3+} quenches the luminescence of the lanthanide ions (Figure 6). The applicability to real samples is confirmed by quantitation of H_2O_2 in spiked urine samples in the range of 0 to 1 mM with good recovery and precision.

Figure 6. Luminescence response of lanthanide coordination polymer nanoparticles to H_2O_2. Reproduced from [21] with permission of The Royal Society of Chemistry.
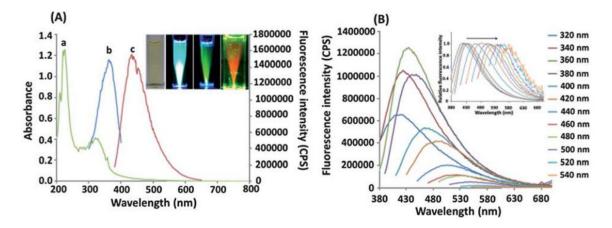
The use of upconversion photoluminescence (UCPL; an anti-Stokes emission) of nanoparticles avoids many disadvantages associated with fluorescence measurements in biological media like scattered light, autofluorescence and photobleaching. This results in high sensitivity and low damage to samples (due to the NIR excitation) when using UCPL for the simultaneous detection of H_2O_2 and glucose in human blood [22]. The approach is based on the selective quenching of the green UCPL of $NaYF_4$ nanoparticles co-doped with Yb^{3+} and Er^{3+} ($NaYF_4$:Yb^{3+}/Er^{3+}) by blue 3,3′,5,5′-tetramethylbenzidine (TMB). TMB is oxidized by H_2O_2 in presence of HRP and its blue oxidation product decreases both the red (659 nm) and the green UCPL (543 nm) of the $NaYF_4$:Yb^{3+}/Er^{3+} nanoparticles. H_2O_2 could be detected from 0.1–4 μM with a 45 nM LOD (λ_{exc} = 543 nm, λ_{em} = 980 nm). Upon coupling, the $NaYF_4$:Yb^{3+}/Er^{3+}-TMB system with glucose oxidase (GOx)-based oxidation of glucose into H_2O_2, a sensitive glucose assay was set up. Concentrations in the range of 0.1–5.0 μM with a LOD of 64.0 nM in diluted human serum were found and satisfactorily validated against a clinical method.

2.6. Carbon Based Nanomaterials

Extraordinary electrical, chemical, optical, mechanical and structural properties of graphene and its derivatives have stimulated the exploration of their potential sensor applications [33]. Moreover, carbon materials are chemically inert and thus low toxic in most cases. However, there are not so many examples of using carbon materials in H_2O_2 sensing. Water-soluble carbon nanodots (C-dots) were prepared using a hydrothermal method and characterized by [23]. These C-dots were used as a fluorescence probe for the quenchiometric detection of H_2O_2 at 410 nm (λ_{exc} = 330 nm) in the presence of Fe^{2+} in a Fenton-like mixture. Moreover, glucose could be monitored via the amount of the enzymatically generated H_2O_2. Upon comparing the C-dot-based detection of H_2O_2 (and glucose) with other methods using metallic clusters and/or QDs as probes, the proposed method seems to be more ecofriendly, has a large (0.025–50 μM) dynamic range and works at a low pH of 3.

The facile one-step pyrolysis of L-glutamic acid can yield nitrogen-doped graphene quantum dots (GQDs) that are highly fluorescent and have an intrinsic peroxidase-like catalytic activity [24]. The GQDs display various fluorescence peaks the main one being at 440 nm (λ_{exc} = 360 nm) and a near-infrared fluorescence (NIR) at >800 nm depending on the excitation wavelength (Figure 7). All lifetimes (measured at different emission wavelengths) are about 2 ns. The peroxidase-like catalytic

activity was used for the colorimetric detection of H_2O_2 in presence of 2,2′-azino-bis(3-ethylbenzothiazoline-6-sulphonic acid) (ABTS). The reduction of H_2O_2 at low mM concentrations (10 mM Tris–HCl pH 5.0, 37 °C) by the GQDs is accompanied by a color change (λ = 416 nm) to green in the presence of ABTS.

Figure 7. (**A**) Absorption (a), excitation (b) and emission spectra (c) of nitrogen-doped GQDs showing an intrinsic peroxidase-like catalytic activity. Inset: (from left to right) GQD solutions under bright light, violet, blue and green irradiation, respectively; (**B**) Luminescence emission spectra of the GQDs with different excitation wavelengths. Reproduced from [24] with permission of The Royal Society of Chemistry.

Another group [25] used GQDs that had adsorbed hemin by π-π stacking and electrostatic interactions. H_2O_2 oxidizes surface-bound hemin, which leads to luminescence quenching of the 471 nm emission concomitantly with a decrease of the absorption at 362 nm. The reaction requires 10 min at room temperature and pH 7.0 (in 20 mM PBS) and additional 30 min of pre-incubation at 37 °C, if coupled to GOx for glucose detection. Glucose can then be detected in concentrations very similar to those of H_2O_2. Validation of glucose levels found in human serum samples against those obtained with a spectrophotometric method yielded a good agreement. The GQDs show the advantages of carbon nanodot materials with respect to environmental and health amenity and therefore seem to be promising for applications in the clinical field.

Carboxyl-functionalized multiwalled carbon nanotubes (MWNTs) were covalently conjugated to HRP to build a hydrogen peroxide biosensor [26]. First, the initial rate of the decomposition of H_2O_2 was calculated from the change of the absorption at 470 nm. The rate of the concentration dependence in mM H_2O_2 s^{-1} nM^{-1} HRP was calculated and used for calibrating the fluorescence measurements. The activity of the enzyme was then determined by measuring the fluorescence of tetraguaiacol at 350 nm, which is released as a colored product from HRP by oxidation of guaiacol as a function of time. The hydrogen peroxide biosensor exhibited a detection limit of 1.2 μM H_2O_2 s^{-1} and hence provided an increased resolution compared to the solution assay by a factor of 8.

3. Sensors, Sensing Membranes and Films for H_2O_2 Detection

Much research has been performed over the last few years on the fabrication of new sensor films made from a wide variety of materials. The interest in sensor membranes is due their simple, low-cost

and rapid production. They also permit monitoring analyte concentrations in a flow-through cell over time or in flow injection analysis (FIA). Moreover, screening of analytes in a highly parallelized manner in high-throughput in standard luminescence readers is feasible when using sensor microtiter plates in which sensor foils are deposited on the bottom of each well. Another option is the coating of the tip of an optical fiber with a sensor cocktail so to form an analyte-responsive membrane. This yields sensors with a highly local resolution that are even capable of remote sensing. The various analytical methods using sensor membranes for determination of H_2O_2 are presented in Table 2.
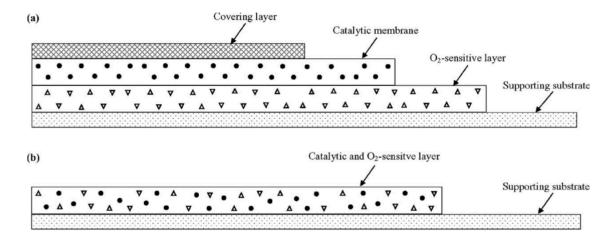
A reversible optical non-enzymatic sensor membrane for H_2O_2 and glucose was described in [34]. The fluorescence of the europium tetracycline complex (EuTc) which is incorporated into a polyacrylonitrile-co-polyacrylamide membrane increases if the sensor membrane is exposed to solutions containing H_2O_2 in concentrations of 0.3–10 mM (5 mM MOPS buffer of pH 6.9). The increase of luminescence at 616 nm (λ_{exc} = 405 nm) is due to a reversible complexation of H_2O_2 to Eu^{3+} in the inner coordination sphere. The coordinative binding of H_2O_2 expels water off the inner coordination sphere and the strong quenching of the luminescence of the lanthanide ion is reduced. The response time is 10 min and the sensor membrane is reversible by flushing with water or (more rapidly) with thiosulfate. Phosphate and citrate and Cu^{2+} interfere in μM concentrations and should therefore be avoided.

Reversible fluorimetric detection of H_2O_2 based on the fluorescence quenching of oxygen sensitive dyes (for example $[Ru(2,2'-bipyridyl)_3]^{2+}$) upon decomposition of H_2O_2 is well-known and was utilized earlier for different types of optical sensors [35]. Voraberger *et al.* [36] used a three layer sensor membrane which has a support made of a poly(ethylene terephthalate). On the top, the oxygen-sensitive $[Ru(dpp)_3]^{2+}(ClO_4)_2]$ complex as the luminophore is coated in polystyrene. Then, a layer of MnO_2 in a silicone membrane is used as catalyst and a polyetherimide is used to prevent water ingress and dye leaching (see Figure 8a). The sensor membrane reversibly responds (t_{90}) within 60 s to 60–300 mM of H_2O_2 detected via luminescence lifetime by the phase-modulation technique upon excitation with a blue LED. The three-layer optode is stable over 5 days. The catalytic membrane is detaching at higher concentrations of hydrogen peroxide which is compensated by addition of an adhesion promoter. The introduction of the catalytic layers increases resistance against harsh chemical conditions and high temperatures which are not accessible with enzymes. The black color of these membranes provides an excellent optical insulation against effects from sample luminescence, background stray light or ambient light.

Recently, a new robust and reversible optical sensor for H_2O_2 was described based on an ion pair containing $[Ru(2,2'-bipyridyl)_3]^{2+}$ as an oxygen probe and RuO_2 as catalyst for the decomposition of H_2O_2. [37]. The luminescence of the dye ion-pair complex with tetraphenylborate $[Ru(bpy)_3(Ph_4B)_2]$ is quenched by O_2 produced by the catalytic breakdown of H_2O_2 utilizing inorganic RuO_2·H_2O as catalyst. The sensor cocktail (coating ink) is just a one-pot formulation that, when dried, forms an active single-layer luminescent H_2O_2 sensor membrane (see Figure 8b). The membrane is less sensitive (10 mM^{-1} M of H_2O_2) compared to the previous sensor but much simpler to be produced. Moreover, the sensor tolerates dry-heat sterilization for 2.5 h in an oven at 150 ℃ without loss of sensitivity. The forward response time (t_{90}) is 309 s and the back response is 98 s (using 455 nm excitation and collecting emission at 585 nm). The sensor works steadily over 40 days (one daily measurement and storage in deionized water), without exhibiting any loss in sensitivity, recovery or response characteristics.

Table 2. Optical Sensor Films for Hydrogen Peroxide.

Composition of Film	Detected Signal	Analytical Range (LOD), mM	Response Time	Conditions and Electrolyte	Ref.
Eu^{3+}-tetracycline complex incorporated into a polyacrylonitrile- polyacrylamide co-polymer	Luminescence increase	0.45–10 (0.45)	10 min	MOPS buffer of pH 6.9 at RT	[34]
[Ru(dpp)$_3^{2+}$] and MnO$_2$ as catalyst	Quenching of luminescence Ru complex due to O$_2$ via phase angle measurement	60–300	1 min	aqueous solutions at 25 ℃	[36]
[Ru(bpy)$_3^{2+}$(Ph$_4$B$_2$)$_2$]	Luminescence quenching of the dye ion-pair due to O$_2$	10–1 × 10^3 (1)	5.2 min	deionized water	[37]
Immobilization of catalase conjugated to O$_2$-sensitive Ru-complex in polyacrylamide	Quenching of luminescence Ru complex due to O$_2$ formation	0.5–14 (0.001)		0.1 M carbonate buffer of pH 9	[38]
Disks of TiO$_2$/SiO$_2$ NP powder in flow-through cell	Phosphorescence quenching due to superoxide coordination to Ti	7 × 10^{-4}–70 1.6 × 10^{-4}	few seconds	water	[39]
HP Green incorporated into a polyurethane polymer	Photoinduced electron transfer of enzymatically oxidized HP Green	0.03–0.3 (8 × 10^{-3})	10 min	10 mM PBS of pH 7.4 at RT	[40]

Figure 8. Composition of a typical (**a**) multilayer sensor membrane as used in [36] and (**b**) of a single-layer sensor membrane for reversible luminescence detection of H_2O_2 via O_2. Former multilayer schemes have the catalyst (•) and luminophore (△) encapsulated in different layers, whereas in [37] a single-layer system catalyst and luminophore are encapsulated in the same polymer matrix. Reproduced from [37] with permission of The Royal Society of Chemistry.

Ortega *et al.* [38] also proposed reversible optical biosensors based on an O_2-sensitive ruthenium complex for continuous monitoring of H_2O_2. Unlike in the previous papers, one bpy ligand of the complex was substituted by 4-methyl-4-carboxy-2,2′-bipyridine to covalently link the complex to catalase (Cat–Ru). After entrapment into a polyacrylamide (PAA) membrane H_2O_2 can be determined after conversion into water and O_2 by action of catalase:

$$H_2O_2 \xrightarrow{\text{Catalase}} H_2O + O_2$$

As an alternative to the sensor membrane a fiber-optical sensor was designed which can be used as immersion probe. The excitation light was produced by a blue LED (450 nm) and the fluorescence intensity was monitored at 600 nm. In both cases, the sensors work in the low mM-range at pH 9 and are fully reversible without chemical regeneration. Organic peroxides show little interferences and the senor shows an operational lifetime for at least one month. The senor behavior was modelled mathematically to allow the judgement on critical experimental parameters. The change of the sensor properties upon use of other luminophores could be predicted, as well. Upon coupling oxidases (which generate H_2O_2) with this catalase-coupled oxygen sensor, access to concentrations of substrates or products of oxidase-type enzymatic reactions is permitted. Potential substrates of interest could be (among glucose) cholesterol, lactic acid, superoxide anions, monoamines and others provided that the enzymes tolerate the conditions required for conjugation with the oxygen probe (20%–44% dimethyl sulfoxide in carbonate buffer pH 8.5).

Shu *et al.* [39] show that a nanoparticular TiO_2/SiO_2-composite obtained from a sol-gel has phosphorescence emission at room temperature at 535 nm when excited at 403 nm. Upon reaction with H_2O_2, superoxide radicals coordinate to Ti as shown by electron spin resonance spectroscopy (ESR). The emission intensity is quenched by H_2O_2 at concentrations over a range of 5 orders of magnitude (7×10^{-7}–7×10^{-2} M) and this is also reflected by the phosphorescence lifetime (3.3–0.4 s). If combined with GOx, glucose can be determined in the mM-range after a few minutes incubation time.

The TiO$_2$/SiO$_2$-composite powder was pressed into round disks that were mounted into a flow-cell. Therein, a very short response time of few seconds towards H$_2$O$_2$ was found and the sensor discs can be used repeatedly using hydroxylamine chloride as reductant. Finally, a semiquantitative determination of H$_2$O$_2$ is possible by eye-vision at mM levels from a color change from white over yellow to orange. The discs were applied to the quantitation of H$_2$O$_2$ in a disinfectant and a contact lens solution as real samples.

A reversible optical sensor microplate was described for high-throughput screening of H$_2$O$_2$ [40]. It uses the fluorescent probe HP Green which is a naphthalimide dye. In presence of H$_2$O$_2$ at physiological pH, the quenched fluorescence of HP Green (by a photoinduced electron transfer (PET)) is terminated. Hence, a rapid "switch-on" of the luminescence at 535 nm (λ_{exc} = 430 nm) is found which is accompanied by an up to eleven-fold increase of the quantum yield [41]. HP Green was incorporated into a polymeric matrix of a D4 polyurethane which was deposited on the bottom of microplate wells. Enzymatic oxidation of HP Green in the presence of HRP enables the determination of H$_2$O$_2$ in the μM-range in solutions of physiological pH. Most notably is the fact that the sensor plate can easily be chemically regenerated with sodium dithionite and reused for quantitation of H$_2$O$_2$ up to five times. The sensor microplate has successfully been applied to the determination of H$_2$O$_2$ in colored cell nutrition medium as a real sample with a strong matrix load.

4. Assessment of Nanomaterials for Potential Use in Optical Sensors

Schemes like sensor membranes, fiber optic sensors or sensor microplates address a promising width of analytical problems from continuous monitoring over high local resolution to remote sensing and high-throughput or multiple sensing. If one compares the fewer sensors published with the much higher numbers of luminescent probes that have been published at the same time, there is a clear difference. The reason is mostly that after having a probe at hand and developed an assay in solution the construction work for a sensor just starts. Here, many additional factors need to be considered like the choice of a supporting material and a suitable polymer (for immobilization of the probe) that also warrants rapid access of the analyte and prevents leaching of the probe. Moreover, the concentration of the probe in the senor film as well as film thickness and layer composition need to be optimized. This still remains to be done for the new nanoparticular materials presented in Section 2 and therefore, this chapter gives suggestions of which ways could be promising to yield a working optical sensor.

The 11-MUA–Au NDs used in [12] are quite promising for building a sensor in that just a ligand binding/unbinding to the NPs is involved in analyte recognition which is connected to an oxidation reaction. As the reversibility of these processes were already demonstrated, the major task to build a sensor would be to find a suitable polymer that is well permeable for small polar analytes to prevent the 11-MUA from leaching off the sensor membrane. Polyurethane polymers like HydroMed D4 [40] are a good example. Then, intermittent addition of a small amount of reductant could regenerate the sensor membrane and provide a repetitive quasi-continuous measurement in certain small intervals. The same regeneration scheme could be useful for [15] where a reductant would need to restore the original size of the HRP-Au NCs. A similar scheme could work for [14] and [22] where repetitive addition of TMB would be required for regeneration. For [21] a complete ligand exchange at the Tb^{3+}-ions would be required to substitute the carboxyphenyl-4-oxo anions with carboxyphenyl-4-

boronic acid groups. The introduction of reversibility is seen to be less easy for other probes [13,16,17] because it would be critical to achieve a reproducible regeneration step *i.e.*, to restore the original particle size and regain the initial luminescence intensity. In case that an enzyme should be co-embedded [15], one might need to consider its lower tolerance towards variations towards buffer, pH and temperature.

QD-based sensors from nanomaterials used in [18] seem possible provided an appropriate surface modification is found that enables a firm anchoring of the particles in the sensor layer. This could be achieved by using copolymers containing nonpolar domains (for particle embedding) and polar domains to allow a rapid access for hydrogen peroxide. Hypan HN80 [42] is a polyacrylamide-polyacrylonitrile copolymer that should be useful for this purpose. It contains hard (polyacrylonitrile domains, lipophilic) and soft blocks (polyacrylamide domains, hydrophilic). Moreover, Hypan can take-up water in fractions up to 80% of its weight and has excellent ion permeability. The reproducible restoring of the particle surface remains an issue to be tested for. The same is true for the C-dots shown in [23]. Here, an intermittent reduction step might be required, as well.

The lanthanide particle probes [20] could be easily embedded into a suitable polymer foil. A continuous operation could be achieved by simultaneously feeding H_2O_2 and the Au-NP growth solution. However, the incubation time for the analytical reaction to proceed would need to become much shorter. The graphene QDs (GQDs) presented in [24] would also require a simultaneous supply of H_2O_2 and ABTS to the QDs immobilized in a sensor foil to then work as a nice continuous sensor both with photometric and luminescence detection.

Another continuous sensing scheme represents flow injection analysis (FIA). Here, reagent solutions and analyte solutions are fed to mixing and detection cells by carrier streams in tubes of few mm of diameter by means of a multichannel peristaltic pump. This could be an option for the assay presented in [25]. Here, the GQDs could premix with and adsorb to hemin in one carrier stream which is then added to the analyte stream. After a further mixing loop, the resulting product stream would be measured via fluorescence spectroscopy. FIA-sensors could also be designed for the nanomaterials presented in [12,14,15,20–22,24] if their synthesis can be easily performed and is not too expensive. The continuous feeding of the nanomaterial as required by a FIA instrument would rise the costs for continuous operation, otherwise.

From all this, it is obvious that sensor design is far beyond having a luminescent probe because it requires careful matching of the properties of many materials, the optical probe and the detection format to yield a system that meets the target figures.

5. Conclusions

This review shows that a wide variety of new luminescent nanomaterials for quantitation of hydrogen peroxide was published over the last five years. These nanomaterials hold great promise for future sensor development. Therefore, the considerable amount of luminescent sensors for H_2O_2 and their various detection formats that have been developed over the past 15 years are discussed. If a sensor is to be developed containing nanomaterials it is frequently important that their surface can be regenerated or reversibly oxidized. Moreover, appropriate embedding of the nanomaterials is required for reliable sensors to be constructed. Hence, additional suggestions of how to fabricate new sensors

for hydrogen peroxide from the nanomaterials are presented. This should inspire scientists to further develop new optical sensors for this important analyte rather than adding just another one to the hundreds of optical glucose assays found in literature. It is therefore desirable that research groups working in probe design and using the many fascinating nanomaterials should acquire additional knowledge in material science to publish new exciting optical sensors for H_2O_2.

Acknowledgments

Author Contributions

Natalia A. Burmistrova and Olga A. Kolontaeva contributed equally to the collection and description of data. Axel Duerkop contributed greatly to the concept, structuring of the work, and to the discussion of the literature cited.

Conflicts of Interest

The authors declare no conflict of interest.

References

1. Winterbourn, C.C. Reconciling the chemistry and biology of reactive oxygen species. *Nat. Chem. Biol.* **2008**, *4*, 278–286.
2. Stamler, J.S.; Singel, D.J.; Loscalzo, J. Biochemistry of nitric oxide and its redox-activated forms. *Science* **1992**, *258*, 1898–1902.
3. Hensley, K.; Robinson, K.A.; Gabbita, S.P.; Salsman, S.; Floyd, R.A. Reactive oxygen species, cell signaling, and cell injury. *Free Radic. Biol. Med.* **2000**, *28*, 1456–1462.
4. Beckman, K.B.; Ames, B.N. The Free Radical Theory of Aging Matures. *Physiol. Rev.* **1998**, *78*, 547–581.
5. Giorgio, M.; Trinel, M.; Migliaccio, E.; Pelicci, P.G. Hydrogen peroxide: A metabolic by product or a common mediator of ageing signals? *Nat. Rev. Mol. Cell Biol.* **2007**, *8*, 722–728.
6. Rhee, S.G. H_2O_2, a Necessary Evil for Cell Signaling. *Science* **2006**, *312*, 1882–1883.
7. D'Autreaux, B.; Toledano, M.B. ROS as signalling molecules: Mechanisms that generate specificity in ROS homeostasis. *Nat. Rev. Mol. Cell Biol.* **2007**, *8*, 813–824.
8. Chen, W.; Cai, S.; Ren, Q.Q.; Wen, W.; Zhao, Y. Recent advances in electrochemical sensing for hydrogen peroxide: A review. *Analyst* **2012**, *137*, 49–58.
9. Chen, S.; Yuan, R.; Chai, Y.; Hu, F. Electrochemical sensing of hydrogen peroxide using metal nanoparticles: A review. *Microchim. Acta* **2013**, *180*, 15–32.
10. Borisov, S.M.; Wolfbeis, O.S. Optical Biosensors. *Chem. Rev.* **2008**, *108*, 423–461.

11. Sch äferling, M.; Gr ögel, D.B.M.; Schreml, S. Luminescent probes for detection and imaging of hydrogen peroxide. *Microchim. Acta* **2011**, *174*, 1–18.

12. Shiang, Y.-C.; Huang, C.-C.; Chang, H.-T. Gold nanodot-based luminescent sensor for the detection of hydrogen peroxide and glucose. *Chem. Commun.* **2009**, *23*, 3437–3439.

13. Lim, S.Y.; Kim, J.H.; Lee, J.S.; Ahn, J.; Kim, M.-G.; Park, C.B. Multi-layered stacks of fluorescent dye-doped silica nanoparticles decorated by gold nanoparticles for solid-phase optical biosensing. *J. Mater. Chem.* **2011**, *21*, 17623–17626.

14. Zhao, Q.; Chen, S.; Huang, H.; Zhang, L.; Wang, L.; Liu, F.; Chen, J.; Zenga, Y.; Chu, P.K. Colorimetric and ultra-sensitive fluorescence resonance energy transfer determination of H_2O_2 and glucose by multi-functional Au nanoclusters. *Analyst* **2014**, *139*, 1498–1503.

15. Wen, F.; Dong, Y.; Feng, L.; Wang, S.; Zhang, S.; Zhang, X. Horseradish Peroxidase Functionalized Fluorescent Gold Nanoclusters for Hydrogen Peroxide Sensing. *Anal. Chem.* **2011**, *83*, 1193–1196.

16. Özalp, V.C.; Zeydanlı, Ü.S.; Lunding, A.; Kavruk, M.; Öz, M.T.; Eyidöğan, F.; Olsend, L.F.; Öktem, H.A. Nanoparticle embedded enzymes for improved lateral flow sensors. *Analyst* **2013**, *138*, 4255–4259.

17. Li, G.; Zhu, D.; Liu, Q.; Xue, L.; Jiang, H. Rapid Detection of Hydrogen Peroxide Based on Aggregation Induced Ratiometric Fluorescence Change. *Org. Lett.* **2013**, *15*, 924–927.

18. Zheng, H.; Su, R.; Gao, Z.; Qi, W.; Huang, R.; Wang, L.; Hea, Z. Magnetic–fluorescent nanocomposites as reusable fluorescence probes for sensitive detection of hydrogen peroxide and glucose. *Anal. Methods* **2014**, *6*, 6352–6357.

19. Adegoke, O.; Khene, S.; Nyokong, T. Fluorescence "Switch on" of Conjugates of CdTe@ZnS Quantum Dots with Al, Ni and Zn Tetraamino-Phthalocyanines by Hydrogen Peroxide: Characterization and Applications as Luminescent Nanosensors. *J. Fluoresc.* **2013**, *23*, 963–974.

20. Li, Z.; Zhang, H.; Shen, J. Preparation of Stable Luminescent Poly(methyl methacrylate)–Europium Complex Nanospheres and Application in the Detection of Hydrogen Peroxide with the Biocatalytic Growth of Gold Nanoparticles. *J. Appl. Polym. Sci.* **2013**, *128*, 845–850.

21. Tan, H.; Ma, C.; Li, Q.; Wang, L.; Xu, F.; Chen, S.; Song, Y. Functionalized lanthanide coordination polymer nanoparticles for selective sensing of hydrogen peroxide in biological fluids. *Analyst* **2014**, *139*, 5516–5522.

22. Liu, J.; Lu, L.; Li, A.; Tang, J.; Wang, S.; Xu, S.; Wang, L. Simultaneous Detection of Hydrogen Peroxide and Glucose in Human Serum with Upconversion Luminescence. *Biosens. Bioelectron.* **2015**, *68*, 204–209.

23. Wei, J.; Qiang, L.; Ren, J.; Ren, X.; Tanga, F.; Meng, X. Fluorescence turn-off detection of hydrogen peroxide and glucose directly using carbon nanodots as probes. *Anal. Methods* **2014**, *6*, 1922–1927.

24. Wu, X.; Tian, F.; Wang, W.; Chen, J.; Wub, M.; Zhao, J.X. Fabrication of highly fluorescent graphene quantum dots using L-glutamic acid for *in vitro*/*in vivo* imaging and sensing. *J. Mater. Chem. C* **2013**, *1*, 4676–4684.

25. He, Y.; Wang, X.; Sun, J.; Jiao, S.; Chen, H.; Gao, F.; Wang, L. Fluorescent blood glucose monitor by hemin-functionalized graphene quantum dots based sensing system. *Anal. Chim. Acta* **2014**, *810*, 71–78.

26. Magyar, M.; Hajdu, K.; Szabó, T.; Endrödi, B.; Hernádi, K.; Horváth, E.; Magrez, A.; Forró, L.; Visy, C.; Nagy, L. Sensing hydrogen peroxide by carbon nanotube/horseradish peroxidase bio-nanocomposite. *Phys. Status Solidi B* **2013**, *250*, 2559–2563.

27. Chen, L.-Y.; Wang, C.-W.; Yuan, Z.; Chang, H.-T. Fluorescent Gold Nanoclusters: Recent Advances in Sensing and Imaging. *Anal. Chem.* **2015**, *87*, 216–229.

28. Déza, I.; Ras, R.H.A. Fluorescent silver nanoclusters. *Nanoscale* **2011**, *3*, 1963–1970.

29. Ansari, S.A.; Husain, Q. Potential applications of enzymes immobilized on/in nano materials: A review. *Biotechnol. Adv.* **2012**, *30*, 512–523.

30. Petryayeva, E.; Algar, W.R; Medintz, I.L. Quantum dots in bioanalysis: A review of applications across various platforms for fluorescence spectroscopy and imaging. *Appl. Spectrosc.* **2013**, *67*, 215–252.

31. Vuojola, J.; Soukka, T. Luminescent lanthanide reporters: New concepts for use in bioanalytical applications. *Methods Appl. Fluoresc.* **2014**, *2*, 012001, doi:10.1088/2050-6120/2/1/012001.

32. Wolfbeis, O.S.; Dürkop, A.; Wu, M.; Lin, Z. Europium Ion-Based Luminescent Sensing Probe for Hydrogen Peroxide. *Angew. Chem. Int. Ed.* **2002**, *41*, 4495–4498.

33. Deng, X.; Tang, H.; Jiang, J. Recent progress in graphene-material-based optical sensors. *Anal. Bioanal. Chem.* **2014**, *406*, 6903–6916.

34. Wolfbeis, O.S.; Schaferling, M.; Dürkop, A. Reversible Optical Sensor Membrane for Hydrogen Peroxide Using an Immobilized Fluorescent Probe, and Its Application to a Glucose Biosensor. *Microchim. Acta* **2003**, *3*, 221–227.

35. Posch, H.E.; Wolfbeis, O.S. Optical sensor for hydrogen peroxide. *Mikrochim. Acta* **1989**, *97*, 41–50.

36. Voraberger, H.S.; Trettnak, W.; Ribitsch, V. Optochemical hydrogen peroxide sensor based on oxygen detection. *Sens. Actuators B Chem.* **2003**, *90*, 324–331.

37. Mills, A.; Tommons, C.; Bailey, R.; Tedford, M.C.; Crilly, P.J. Reversible, fluorescence-based optical sensor for hydrogen peroxide. *Analyst* **2007**, *132*, 566–571.

38. Ortega, E.; de Marcos, S.; Galban, J. Fluorometric enzymatic autoindicating biosensor for H_2O_2 determination based on modified catalase. *Biosens. Bioelectron.* **2013**, *41*, 150–156.

39. Shu, X.; Chen, Y.; Yuan, H.; Gao, S.; Xiao, D. H_2O_2 Sensor Based on the Room-Temperature Phosphorescence of Nano TiO_2/SiO_2 Composite. *Anal. Chem.* **2007**, *79*, 3695–3702.

40. Burmistrova, N.A.; Meier, R.J.; Schreml, S.; Duerkop, A. Reusable optical sensing microplate for hydrogen peroxide using a fluorescent photoinduced electron transfer probe (HP Green). *Sens. Actuators B Chem.* **2014**, *193*, 799–805.

41. Groegel, D.B.M.; Link, M.; Duerkop, A.; Wolfbeis, O.S. A New Fluorescent PET Probe for Hydrogen Peroxide and its Use in Enzymatic Assays for L-Lactate and D-Glucose. *ChemBioChem* **2011**, *12*, 2779–2785.

42. Ast, S.; Schwarze, T.; Müller, H.; Sukhanov, A.; Michaelis, S.; Wegener, J.; Wolfbeis, O.S.; Körzdörfer, T.; Dürkop, A.; Holdt, H.-J. A Highly K^{+}-Selective Phenylaza-[18]crown-6-Lariat-Ether-Based Fluoroionophore and Its Application in the Sensing of K^{+} Ions with an Optical Sensor Film and in Cells. *Chem. Eur. J.* **2013**, *19*, 14911–14917.